

Supplementary: Self-organized defect strings in two-dimensional crystals

Wolfgang Lechner,¹ David Polster,² Georg Maret,² Peter Keim,² and Christoph Dellago³

¹*Institute for Quantum Optics and Quantum Information and Institute for Theoretical Physics, University of Innsbruck, 6020 Innsbruck, Austria*

²*Department of Physics, University of Konstanz, D-78457 Konstanz, Germany*

³*Faculty of Physics, University of Vienna, Boltzmanngasse 5, 1090 Vienna, Austria*

(Dated: September 20, 2013)

In this Supplementary Information we provide some additional technical details about the experiment and the computation of diffusion constants and the identification of defects, as well as a more detailed comparison of our results with the predictions of elasticity theory.

I. EXPERIMENTAL DETAILS

The monolayer consists of polystyrene beads with (4.5 μm diameter) doped with iron oxide (Dynabeads[®] 4.5, Invitrogen) making them superparamagnetic. The beads are sedimented by gravity to an otherwise interaction free interface of a hanging droplet spanned by surface tension in a top sealed cylindrical hole (4 mm in diameter) of an optical cuvette. The thermal activation height (out of plane motion) is less than 20 nm and is therefore neglected. Computer controlled regulation loops counting particle numbers and measuring their size relative to focal plane guarantee the flatness of the water-air interface. This is done by adjusting the volume of the droplet in sub-nanoliter units with a micro-syringe driven by a micro-stage with a frequency of 0.1 Hz. To align the whole setup with respect to gravity the experiment is mounted on a flexible tripod steered by an inclination sensor. This way changes in inclination are suppressed below 10^{-6} rad and spatial density variations are less than 0.1% in the field of view. The monitored area is $863 \times 645 \mu\text{m}^2$ recorded with a CCD-camera of 1392×1040 pixels (Marlin F 145-B), containing about 3000 particles, whereas the whole monolayer consists of up to 5×10^4 particles. An elaborated description of the experimental setup can be found in [1].

II. NUMERICAL DETAILS

The simulated system consists of $M = 52 \times 60 = 3120$ particles in an almost quadratic simulation box with periodic boundary conditions. A cutoff of $r_c = 5.0a$ for the interactions was used together with cell lists to accelerate the simulations. The system is studied with Metropolis Monte Carlo simulations at constant particle number, box size and temperature. Trial moves consist of single particle displacements carried out with a maximum displacement size selected to obtain an average acceptance probability of about 50%. The simulation time scale is mapped to the physical time scale by comparing the self

diffusion constants in the liquid state obtained from simulations and experiments (see Supplementary Information). In all our experiments and simulations $\Gamma = 160$ leading to a Young's modulus of $K = 1.258\Gamma = 201.3$ [2].

III. DIFFUSION

To monitor the long time diffusion of the defect strings, we determine the mean square displacement $\langle \Delta r(t)^2 \rangle = \langle [r(t) - r(0)]^2 \rangle$ of the center of mass r of the string endpoints. The diffusion constant D_{string} is estimated by least square fit to the relation $\langle \Delta r(t)^2 \rangle = 4D_{\text{string}}t$ giving the diffusion constants shown in Fig. 2 of the main text. To relate the physical time and the time scale τ of the simulation corresponding to one Monte Carlo sweep, we have determined the diffusion constant of a particle in the fluid, which is also known experimentally [3, 4]. For $M = 780$ particles and $\Gamma = 40$, the Monte Carlo simulation yields a diffusion constant of $D = 1.69 \pm 0.19 \times 10^{-6} a_0^2/\tau$. From the experimental diffusion constant $D_{\text{exp}} = 0.11 \mu\text{m}^2/\text{s}$ one obtains $\tau = a_0^2/(0.11 \mu\text{m}^2/\text{s})$ for the time scale of the simulation.

IV. DEFECT IDENTIFICATIONS

A quantitative description of the dynamics of defect strings requires the accurate identification and location of dislocations and vacancies. Here, we identify dislocations as pairs of particles with 5 and 7 neighbors, respectively [5]. Neighbor numbers are determined using a Voronoi analysis [6]. The position of a dislocation is defined to be at the center of mass of the 5- and 7-coordinated particles and the Burgers vector of the dislocation is orthogonal to the vector pointing from the 5- to the 7-coordinated particle. Single vacancies can, in principle, also be identified from the position of the dislocations associated with them [7]. However, if vacancies form a cluster, some dislocations annihilate and the individual positions of the defects can not be resolved any longer. Here, we identify vacancies based on a underlying reference lattice consisting of a perfect triangular crystal with the density of the defect free crystal. The defect identification consist of the following steps: Each particle is first assigned to its closest perfect lattice site. The perfect lattice is then positioned to minimize the sum of distances between particles and the assigned lattice sites. With this step, the

lattice follows the center-of-mass motion of the crystal. The positions of the vacancies are then identified as the position of unoccupied lattice sites. This procedure to locate vacancies is robust and the number of vacancies is constant throughout the simulation even if the vacancies assemble into a string.

As explained in the main text, the dynamics of vacancy strings consist of long gliding periods interrupted by rotation events at which the direction of motion of the string changes. The rotation rate $k_{\text{rot}} = N_{\text{rot}}/t$ is the number N_{rot} of rotation events that have occurred during the time t . To determine the rotation rate, we identify the orientation of the strings at each time step and detect rotation events based on changes in the string orientation. The string orientation is defined by the relative position of the dislocations that terminate the strings and it coincides with the direction of the Burgers vectors. The string orientation is undefined at the rotation points, where the string can change between two orientations.

V. DISLOCATION INTERACTION

According to linear elasticity theory, the interaction energy of two dislocations with Burgers vectors \mathbf{b}_1 and \mathbf{b}_2 and separated by \mathbf{R} is given by [8]

$$\beta F = -\frac{K}{4\pi} \left[(\mathbf{b}_1 \cdot \mathbf{b}_2) \ln R - \frac{(\mathbf{b}_1 \cdot \mathbf{R})(\mathbf{b}_2 \cdot \mathbf{R})}{R^2} \right], \quad (1)$$

where K is Young's modulus and $\beta = 1/k_{\text{B}}T$. In a coordinate system with x -axis in the direction of motion, the separation vector for a string of N vacancies can be written as $\mathbf{R} = (s, N\sqrt{3}/2)$ and the Burgers vectors are given $\mathbf{b}_1 = (-1, 0)$, $\mathbf{b}_2 = (1, 0)$. Using the dimensionless variable $x = 2s/(\sqrt{3}N)$ one then obtains

$$\beta F(x) = \frac{K}{8\pi} \left(\frac{1-x^2}{1+x^2} + \ln \frac{1+x^2}{2} \right), \quad (2)$$

where the free energy has been shifted to vanish at its minimum value. This function has the shape of a symmetric double well with minima located at $x = \pm 1$. The minima are separated by a barrier of height $h = (K/8\pi)(1 - \ln 2)$ at $x = 0$. As shown in Fig. 3 of the main paper, the effective dislocation interactions extracted from our experiments and simulations display the double-well form predicted by elasticity theory for sufficiently long strings. A more detailed comparison is provided in the following.

The positions x of the minima obtained from the experiment and simulations are depicted in Fig. 1 together with the prediction of elasticity theory shown as horizontal line. For strings of more than $N > 3$ vacancies, both experiment and simulation agree very well with elasticity theory. For short strings with $N \leq 3$, however, the double-well form disappears and the minimum shifts to $x = 0$.

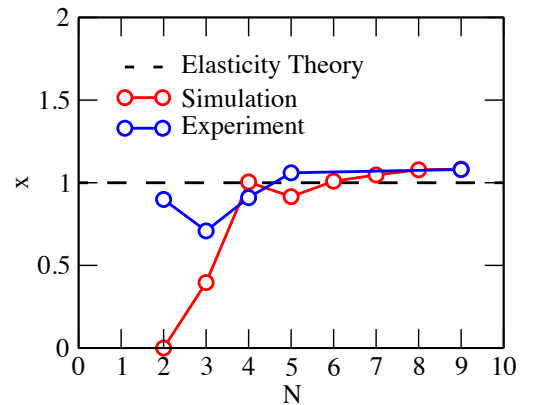


FIG. 1: Position x of the local minima as a function of string length N obtained from simulations (red) and experiments (blue). For $N > 3$ the prediction of elasticity theory (black horizontal line) is in excellent agreement with experiment and simulations.

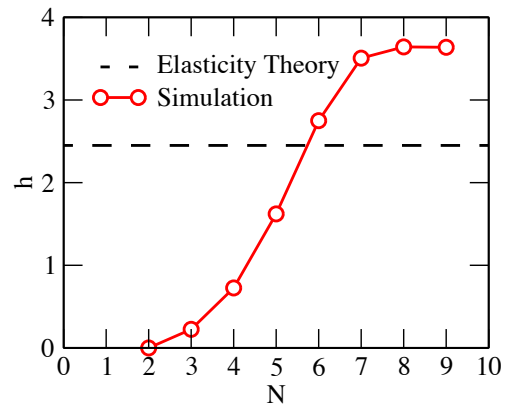


FIG. 2: Barrier height h obtained as a function of the string length N from simulations (red) compared to the predictions of elasticity theory (black horizontal line). While for short strings the barrier disappears, for long strings it converges to a constant value which exceeds the prediction of elasticity theory by about 50%.

Barrier heights h obtained for different string lengths N are depicted in Fig. 2. Since the statistics of the experimental measurements are insufficient for an accurate determination of barrier heights, only simulation results are shown. While elasticity theory predicts a barrier height of $h = 2.45k_{\text{B}}T$ independent of string length, the barrier height determined in our simulations vanishes for $N = 2$ and then grows with string length until it converges to a constant value for strings consisting of more than about $N = 7$ vacancies. The barrier height obtained for long strings exceeds the elasticity theory value by about 50%. While one expects elasticity theory to break down at small distances, the origin of this discrepancy observed in the long string limit is unclear and might be due to

non-linear interactions.

- [1] F. Ebert, P. Dillman, G. Maret, and P. Keim, *Rev. Sci. Instrum.* **80**, 083902 (2009).
- [2] H. H. von Grünberg, P. Keim, K. Zahn, and G. Maret, *Phys. Rev. Lett.* **93**, 255703 (2004).
- [3] K. Zahn, J. M. Méndez-Alcaraz, and G. Maret, *Phys. Rev. Lett.* **79**, 175 (1997).
- [4] B. Rinn , K. Zahn, P. Maass and G. Maret, *Europhys. Lett.* **46**, 537 (1999).
- [5] C. Eisenmann, U. Gasser, P. Keim, G. Maret, H.-H. von Grünberg, *Phys. Rev. Lett.* **95**, 185502 (2005).
- [6] S. Fortune, *Algorithmica* **2**, 153 (1987).
- [7] W. Lechner and C. Dellago, *Soft Matter*, **5**, 646 (2009).
- [8] F. Nabarro, “Theory of Dislocations”, Clarendon, Oxford (1967).